dynamics associated with the neutral I atom have not been considered.

We close by comparing our results to Bradforth's experiments (*11*) on CTTS excitation of I^- in liquid water, because these are the liquid-phase experiments most analogous to ours. In his experiments, transient absorption at 800 nm was monitored after excitation at 255 nm. Bradforth observed a short-lived (~50 fs) transient assigned to the initially excited CTTS state, followed by an increasing absorption with a rise time of 200 fs associated with formation of the solvated electron; this then decayed biexponentially with time constants of 9 and 60 ps. This interpretation suggests several parallels with the $n = 5$ and $n = 6$ FPES results presented here; namely that the CTTS state in the bulk is analogous to the short-lived dipole-bound state seen in our experiments, and that the bulk solvation on a 200-fs time scale corresponds to the isomerization and solvation dynamics in our experiments. There are, however, important differences. Simulations of CTTS excitation show that solvation is accompanied by the electron moving away from the halogen species (*12, 13*), which is a reasonable result for an infinite number of water molecules but may not occur in a small cluster. Also, in liquid water, the longer time decay of the solvated electron signal occurs by recombination with neutral I atoms. Although this may be responsible for the long time decay in the clusters, a likelier mechanism is thermionic emission, which generally does not occur in liquids.

References and Notes

1. W. Weyl, *Poyg. Ann.* **123**, 350 (1864).
2. E. J. Hart and J. W. Boag, *J. Am. Chem. Soc.* **84**, 4090 (1962).
3. M. Wiesenfeld and E. P. Ippen, *Chem. Phys. Lett.* **73**, 47 (1980); A. Migus, Y. Gauduel, J. L. Martin, A. Antonetti, *Phys. Rev. Lett.* **58**, 1559 (1987).
4. C. Silva, P. K. Walhout, K. Yokoyama, P. F. Barbara, *Phys. Rev. Lett.* **80**, 1086 (1998).
5. B. J. Greenblatt, M. T. Zanni, D. M. Neumark, *Chem. Phys. Lett.* **258**, 523 (1996).
6. B. J. Greenblatt, M. T. Zanni, D. M. Neumark, *Science* **276**, 1675 (1997).
7. J. Franck and G. Scheibe, *Z. Phys. Chem. A* **139**, 22 (1928).
8. J. Jortner, M. Ottolenghi, G. Stein, *J. Phys. Chem.* **68**, 247 (1964).
9. F. H. Long, X. Shi, H. Lu, K. B. Eisenthal, *ibid.* **98**, 7252 (1994).
10. Y. Gaudeul, H. Gelabert, M. Ashokkumar, *Chem. Phys.* **197**, 167 (1995).
11. J. A. Kloepfer, V. H. Vilchiz, V. A. Lenchenkov, S. E. Bradforth, *Chem. Phys. Lett.* **298**, 120 (1998).
12. W.-S. Sheu and P. J. Rossky, *ibid.* **213**, 233 (1993).
13. A. Staib and D. Borgis, *J. Chem. Phys.* **104**, 9027 (1996).
14. D. Serxner, C. E. Dessent, M. A. Johnson, *ibid.* **105**, 7231 (1996).
15. B. J. Greenblatt, M. T. Zanni, D. M. Neumark, *Disc. Faraday Soc.* **108**, 101 (1997).
16. Briefly, a pulsed beam of cold $I^-(D_2O)_n$ anion clusters is formed by crossing an electron beam with a pulsed supersonic expansion of a gas mixture of about 5% CH_3I and 2% D_2O (or H_2O) in 1 bar N_2 into a vacuum chamber. The resulting anions are mass selected by time of flight and interact with the pump and probe laser pulses at the focus of a "magnetic bottle" time-of-flight PE spectrometer. The pump and probe laser pulses were generated by a Ti:sapphire oscillator-regenerative amplifier system (Clark MXR) running at a repetition rate of 500 Hz.
17. J. E. Combariza, N. R. Kestner, J. Jortner, *J. Chem. Phys.* **100**, 2851 (1994); *Chem. Phys. Lett.* **221**, 156 (1994).
18. L. Perera and M. Berkowitz, *J. Chem. Phys.* **100**, 3085 (1994).
19. S. S. Xantheas, *J. Phys. Chem.* **100**, 9703 (1996).
20. G. Markovich, S. Pollack, R. Giniger, O. Cheshnovsky, *J. Chem. Phys.* **101**, 9344 (1994).
21. O. H. Crawford, *Mol. Phys.* **20**, 585 (1971).
22. T. R. Taylor, H. Gomez, D. M. Neumark, in preparation.
23. J. V. Coe *et al.*, *J. Chem. Phys.* **92**, 3980 (1990); J. H. Hendricks *et al.*, in *Structure and Dynamics of Clusters*, T. Kondow, K. Kaya, A. Terasaki, Eds. (Universal Academy Press, Tokyo, 1996), pp. 321–328.
24. C. G. Bailey and M. A. Johnson, *Chem. Phys. Lett.* **265**, 185 (1997).
25. S. Lee, J. Kim, S. J. Lee, K. S. Kim, *Phys. Rev. Lett.* **79**, 2038 (1997).
26. P. Ayotte *et al.*, *Chem. Phys.* **239**, 485 (1998).
27. P. Ayotte *et al.*, *J. Chem. Phys.* **110**, 6268 (1999).

28. Supported by the Air Force Office of Scientific Research under grant F49620-97-0018. R.W. acknowledges funding by the Deutsche Forschungsgemeinschaft. C.F. acknowledges postdoctoral support from the Deutsche Akademie der Naturforscher Leopoldina (grant BMBF-LPD 9801-6). L.L. acknowledges financial support by E. W. Schlag.

18 December 1998; accepted 16 March 1999

Requirement for Tec Kinases Rlk and Itk in T Cell Receptor Signaling and Immunity

Edward M. Schaeffer,[1]* Jayanta Debnath,[1,2]*† George Yap,[3] Daniel McVicar,[2] X. Charlene Liao,[4] Dan R. Littman,[5] Alan Sher,[3] Harold E. Varmus,[2] Michael J. Lenardo,[3] Pamela L. Schwartzberg[1,2]‡

T cell receptor (TCR) signaling requires activation of Zap-70 and Src family tyrosine kinases, but requirements for other tyrosine kinases are less clear. Combined deletion in mice of two Tec kinases, Rlk and Itk, caused marked defects in TCR responses including proliferation, cytokine production, and apoptosis in vitro and adaptive immune responses to *Toxoplasma gondii* in vivo. Molecular events immediately downstream from the TCR were intact in $rlk^{-/-}itk^{-/-}$ cells, but intermediate events including inositol trisphosphate production, calcium mobilization, and mitogen-activated protein kinase activation were impaired, establishing Tec kinases as critical regulators of TCR signaling required for phospholipase C–γ activation.

Stimulation of T lymphocytes through the TCR elicits broad responses required for proper immune function, including cell proliferation, cytokine production, and apoptosis. Key components of TCR signaling are nonreceptor tyrosine kinases, and cells lacking Lck or Zap-70 are essentially unresponsive to antigen (*1*, *2*). The Tec kinases, exemplified by BTK, are a distinct family with members specifically expressed in lymphoid lineages (*3*, *4*). *BTK* mutations cause severe immunodeficiencies, with defective B cell development and function (*4*). No disease is yet associated with the loss of Tec kinases in T lymphocytes, which express Itk, Rlk, and Tec (*3*). Itk-deficient mice have only mildly impaired responses to infection (*5*), suggesting functional redundancy between these kinases.

Rlk (also called Txk) is a Tec kinase expressed in developing and mature T lymphocytes (*6*). Rlk resembles other Tec kinases in that it lacks the COOH-terminal regulatory tyrosine and myristoylation sequences of Src kinases, has a proline-rich region that binds SH3 domains, and is activated by phosphorylation by Src kinases. However, Rlk lacks the phosphatidylinositol phosphate–binding pleckstrin homology domain common to other Tec kinases and is activated independently of phosphoinositide 3-kinase (PI3K) activity. Instead, Rlk has a palmitoylated cysteine-string motif, required for subcellular localization (*7*). To better understand the contribution of Tec kinases to T cell signaling, we analyzed mice mutated in Rlk, Itk, or both kinases.

Because alternate translation initiation generates at least two Rlk isoforms, a full-length protein and a shorter species lacking the cysteine string (*7*), we introduced a targeted mutation downstream of the second

[1]National Human Genome Research Institute, [2]National Cancer Institute, [3]National Institute for Allergy and Infectious Diseases, NIH, Bethesda, MD 20892, USA. [4]Tularik, 2 Corporate Drive, South San Francisco, CA 94080, USA. [5]Skirball Institute of Biomolecular Medicine, NYU Medical Center, 540 First Avenue, New York, NY 10016, USA.

*These authors contributed equally to this work.
†Present address: Department of Pathology, Brigham and Women's Hospital, 75 Francis Street, Boston, MA 02115, USA.
‡To whom correspondence should be addressed. E-mail: pams@nhgri.nih.gov

initiation codon of *rlk* into mouse embryonic stem (ES) cells (Fig. 1, A and B). Heterozygous F_1 offspring of chimeric mice were interbred and generated normal numbers of homozygous *rlk* mutants with no evidence of kinase-active Rlk or truncated Rlk protein species in lymphoid cell extracts (Fig. 1C). Preliminary analyses of these mice suggested that all thymocyte and mature T cell populations were present with no major defects in T cell functional responses in vitro (see below).

Northern blot analyses of RNA from lymphoid organs of $rlk^{-/-}$ mice showed slightly increased amounts of *itk* mRNA (*8*). Thus, up-regulation of related Tec kinases may partially compensate for the lack of Rlk. To address this possibility, we generated $rlk^{-/-}itk^{-/-}$ mice by interbreeding. Itk-deficient mice have reduced numbers of mature T cells, particularly $CD4^+$ cells, causing a decreased CD4:CD8 ratio (*9*). $rlk^{-/-}itk^{-/-}$ mutants, however, had normal total T cell numbers (Fig. 1D). Both $CD4^+$ and $CD8^+$ cell numbers are increased relative to $itk^{-/-}$ mice; therefore, $rlk^{-/-}itk^{-/-}$ animals still have a decreased CD4:CD8 ratio (Fig. 1D), suggesting altered regulation of lymphoid development and homeostasis (*10*).

Although $rlk^{-/-}itk^{-/-}$ mice have mature T cells, these cells failed to respond to TCR activation as measured by proliferation of splenocytes stimulated with antibody to CD3ε (anti-CD3ε) (Fig. 2A) or concanavalin A (Con A) (*8*). This defect was confirmed with purified T cells in the presence of irradiated wild-type antigen-presenting cells and in mixed lymphocyte reactions (*8*). In contrast to $itk^{-/-}$ cells, which have only variable defects in $CD4^+$ cell proliferation (*9*), $rlk^{-/-}itk^{-/-}$ cells had proliferative defects in both $CD4^+$ and $CD8^+$ T cell populations (*8*). Treatment with phorbol myristate acid (PMA) and the calcium ionophore ionomycin induced proliferation equivalent to that of wild-type cells, suggesting that defects in these cells lie proximal to Ca^{2+} mobilization and protein kinase C (PKC) activation.

Splenocytes from $rlk^{-/-}$ animals stimulated in vitro with either anti-CD3ε or anti–Con A secreted half the interleukin 2 (IL-2) produced by wild-type animals, whereas $itk^{-/-}$ cells had more severe reductions in IL-2 production, as previously reported (*9*, *11*). However, deficiency of both kinases further reduced IL-2 and interferon-γ (IFN-γ) production to undetectable levels (Fig. 2B). Furthermore, proliferation of $rlk^{-/-}itk^{-/-}$ cells was only partially restored by exogenous IL-2 (Fig. 2A), probably as a result of defective up-regulation of IL-2 receptor-α chain (CD25) (Fig. 2C), even in the presence of exogenous IL-2 (*8*). We also observed decreased TCR-driven apoptosis, an important component of T cell homeostasis (Fig. 2D) (*12*), suggesting one mechanism for increased T cell numbers in $rlk^{-/-}itk^{-/-}$ mice relative to $itk^{-/-}$ animals.

To investigate biochemical defects in $rlk^{-/-}itk^{-/-}$ T cells, we examined signaling events downstream of the TCR. Patterns of CD3-mediated tyrosine phosphorylation were not grossly altered, and the most proximal consequences of T cell activation, including phosphorylation of TCR zeta chains and Zap-70 (*1*), were intact in all genotypes (Fig. 3A).

In contrast, Ca^{2+} mobilization upon T cell activation (Fig. 3B) was reduced in $itk^{-/-}$ cells (*11*) and substantially worsened by deficiency of both Itk and Rlk. Ca^{2+} mobilization in T cells is initiated by membrane association and activation of phospholipase C–γ (PLC-γ), which catalyzes the breakdown of phosphatidylinositol-4,5-bisphosphate into inositol trisphosphate (IP_3), a stimulant for Ca^{2+} mobilization, and diacylglycerol (DG), an activator of PKC (*13*). Within 2 min of TCR stimulation, tyrosine phosphorylation of PLC-γ was observed in wild-type cells, but not in $rlk^{-/-}itk^{-/-}$ or $itk^{-/-}$ T cells (Fig. 3C). However, 5 min after stimulation, PLC-γ was phosphorylated in both wild-type and mutant cells, with only a fewfold reduction in $rlk^{-/-}itk^{-/-}$ cells. Wild-type cells also showed maximal IP_3 levels at 2 to 3 min after stimulation, consistent with rapid phosphorylation of PLC-γ and peak Ca^{2+} mobilization. In contrast, double knockout cells produced virtually no IP_3, even at time points when PLC-γ phosphorylation was observed (Fig. 3D). Our results suggest that only early PLC-γ tyrosine

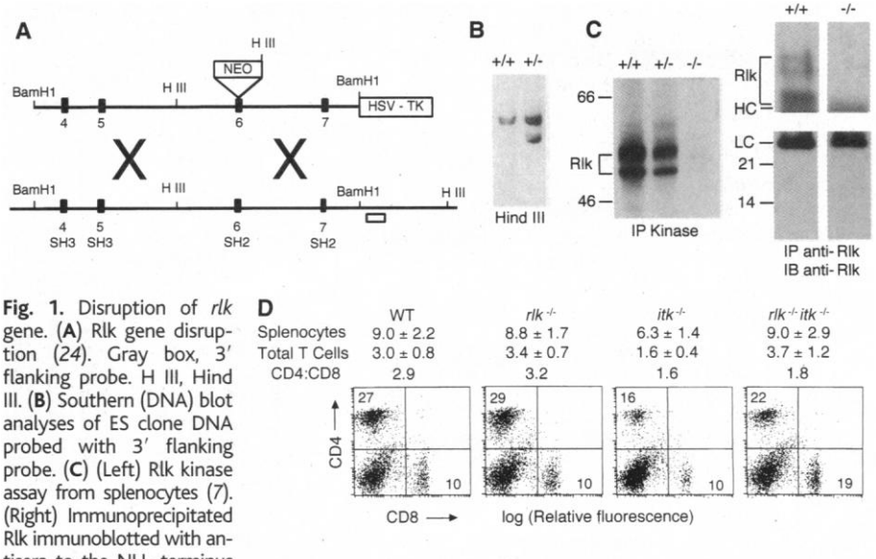

Fig. 1. Disruption of *rlk* gene. (**A**) Rlk gene disruption (*24*). Gray box, 3′ flanking probe. H III, Hind III. (**B**) Southern (DNA) blot analyses of ES clone DNA probed with 3′ flanking probe. (**C**) (Left) Rlk kinase assay from splenocytes (*7*). (Right) Immunoprecipitated Rlk immunoblotted with antisera to the NH_2-terminus of Rlk. Samples were resolved by 10% SDS-PAGE for full-length Rlk (top panels) and by 4 to 20% SDS-PAGE for smaller protein species (predicted truncated products of 16 and 10 kD, bottom panels). IP, immunoprecipitation; IB, immunoblot; HC, heavy chain; LC, light chain. Numbers at left indicate the molecular mass (in kilodaltons). (**D**) $CD4^+$ and $CD8^+$ splenic T cell subsets. Cellularity of spleens ($\times 10^7$) and percentage of $CD4^+$ and $CD8^+$ cells represent the average of 7 to 12 mice per genotype. Flow cytometric antibodies were obtained from PharMingen.

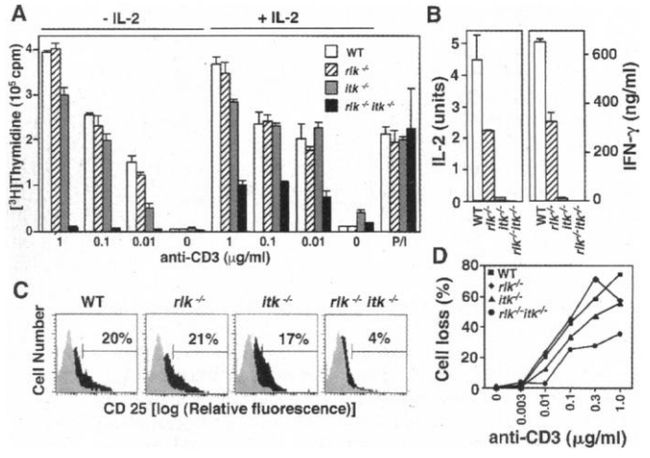

Fig. 2. Disruption of Rlk and Itk impairs T cell functional responses. (**A**) Proliferative defects. Total splenocytes stimulated with 2C11 (anti-CD3ε) with or without exogenous recombinant human IL-2 (100 U/ml; Parke-Davis) or PMA (10 ng/ml) and ionomycin (1 μg/ml) (P/I) for 40 to 48 hours were pulsed with [^{3}H]thymidine and harvested after 6 to 12 hours. (**B**) IL-2 and IFN-γ levels after stimulation of splenocytes with anti-CD3 (3 μg/ml) for 24 hours measured by enzyme-linked immunosorbent assay (ELISA). (**C**) CD25 expression after stimulation of splenocytes with 2C11. Baseline CD25 expression is in gray. WT, wild type. (**D**) TCR-mediated apoptosis (*25*).

phosphorylation correlates with IP_3 production and that this defect may be the major cause of altered Ca^{2+} mobilization in $rlk^{-/-}itk^{-/-}$ cells.

DG, the other product of PLC-γ, activates mitogen-activated protein (MAP) kinases ERK1 and ERK2 through PKC stimulation of the Ras/Raf pathway (*14*). Decreases in phosphorylated (active) ERK1 and ERK2 were also observed after anti-CD3 stimulation of T cells from both $itk^{-/-}$ and $rlk^{-/-}itk^{-/-}$ mice (Fig. 3E) (*15*). To specifically examine DG-mediated MAP kinase activation, we stimulated cells with anti-CD3 and low concentrations of PMA, a phorbol ester that directly activates PKC. Anti-CD3 plus PMA rescued proliferation in $rlk^{-/-}itk^{-/-}$ cells (Fig. 3F) and normalized activation of ERK1 and ERK2 (*8*). Hence, the defective MAP kinase activation in $rlk^{-/-}itk^{-/-}$ cells probably results from defects in DG-PKC–mediated pathways (*16*). Similarly, ionomycin also partially bypasses $rlk^{-/-}itk^{-/-}$ defects in CD3-driven proliferation (*8*). Thus, Tec family kinases are critical in TCR signaling for full activation of PLC-γ and both arms of its downstream effector pathways.

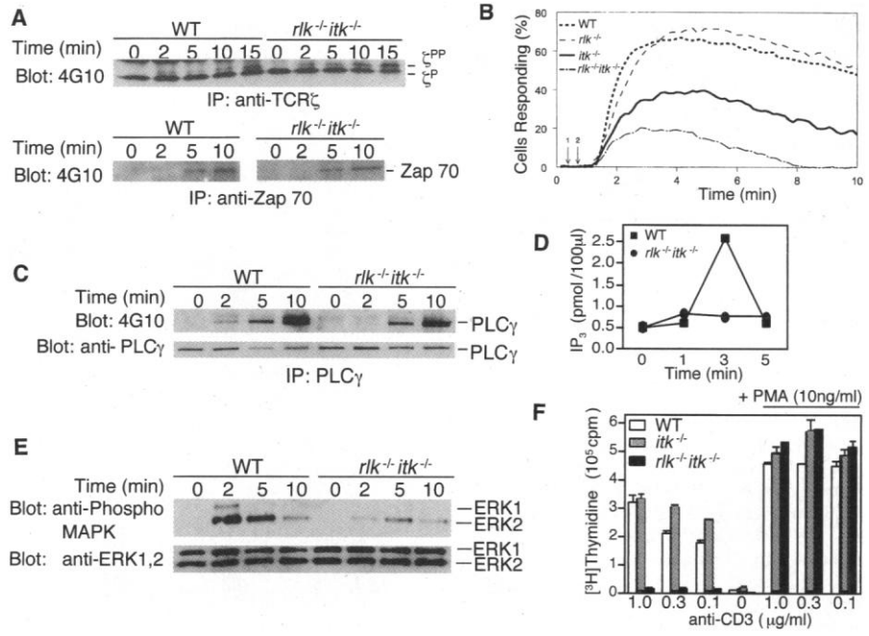

Fig. 3. Ca^{2+} and MAP kinase pathways in $rlk^{-/-}itk^{-/-}$ mice. (**A**) Tyrosine phosphorylation of TCR zeta chain and Zap-70 in response to TCR stimulation (*23*). (**B**) Calcium flux in response to TCR stimulation (*26*). First arrow designates addition of biotinylated 2C11 and second arrow denotes cross-linking with streptavidin. (**C**) PLC-γ phosphorylation. Lysates from 2C11-stimulated purified T cells (5×10^6) were immunoprecipitated with anti–PLC-γ (Upstate), immunoblotted with anti-phosphotyrosine, and then reprobed with anti–PLC-γ. (**D**) IP_3 production (*27*). (**E**) MAP kinase (MAPK) activation. Total cell lysates were resolved by SDS-PAGE (4 to 20% gradient) and probed sequentially with anti–phospho-MAPK that detects dually phosphorylated (active) ERK1 and ERK2 and anti-ERK1 (Santa Cruz) that recognizes ERK1 and ERK2. (**F**) T cell proliferation in response to anti-TCR and PMA. Proliferation was assayed as in Fig. 2A.

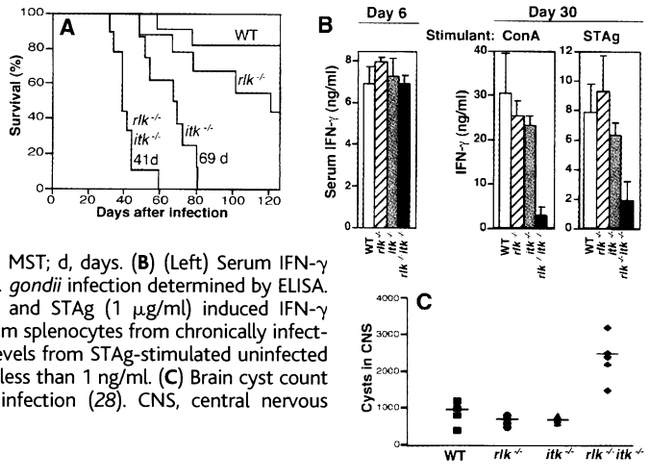

Fig. 4. Impaired resistance to *T. gondi*. Mice were infected intraperitoneally with 20 cysts of *T. gondii* (ME49 strain). (**A**) Survival curves. Pooled data from two independent infections (wild type, $n = 11$; $rlk^{-/-}$ and $rlk^{-/-}itk^{-/-}$, $n = 9$; $itk^{-/-}$, $n = 8$). Numbers indicate MST; d, days. (**B**) (Left) Serum IFN-γ levels 6 days after acute *T. gondii* infection determined by ELISA. (Right) Con A (3 μg/ml) and STAg (1 μg/ml) induced IFN-γ production at 48 hours from splenocytes from chronically infected (day 30) mice. IFN-γ levels from STAg-stimulated uninfected wild-type splenocytes are less than 1 ng/ml. (**C**) Brain cyst count 30 days after *T. gondii* infection (*28*). CNS, central nervous system.

To assess whether these in vitro defects translate into immunodeficiency in vivo, we challenged the Tec kinase–deficient mice with the intracellular pathogen *Toxoplasma gondii*. Mice of all mutant genotypes survived early infection, which requires natural killer (NK) cell activity, suggesting normal innate immunity (Fig. 4A) (*17*). However, 30 days after infection, $rlk^{-/-}itk^{-/-}$ mice appeared visibly ill and had a mean survival time (MST) of 41 days. Itk-deficient animals died with an MST of 69 days, whereas only half of $rlk^{-/-}$ animals had succumbed by 102 days. In these experiments, 80% of wild-type animals in the same genetic background survived over 18 weeks (126 days; Fig. 4A). These results suggest a graded resistance to *T. gondii* that correlates with expression of Tec family kinases.

Correspondingly, serum IFN-γ concentrations 5 days after infection were normal in mice of all genotypes, suggesting unimpaired NK cell function (Fig. 4B). In contrast, splenocytes from $rlk^{-/-}itk^{-/-}$ mice 30 days after infection cultured with Con A or low-dose soluble tachyzoite antigen (STAg) produced decreased IFN-γ (Fig. 4B), indicating a deficit in adaptive antigen-driven responses, consistent with decreased cytokine production in naïve $rlk^{-/-}itk^{-/-}$ T cells (see Fig. 2B). Itk-deficient splenocytes had near normal IFN-γ production in response to these stimuli, thereby demonstrating increased responsiveness of $itk^{-/-}$ cells after in vivo challenge (see Fig. 2B). Finally, 30 days after infection, $rlk^{-/-}itk^{-/-}$ mice had increased brain cyst numbers, indicating decreased ability to limit infection at this T cell–dependent stage (Fig. 4C). Thus, the enhanced susceptibility of $rlk^{-/-}itk^{-/-}$ mice to *T. gondii* demonstrates the physiologic importance in vivo of the marked defects observed in vitro.

Together, the above biological and biochemical evidence demonstrates that Tec family kinases are essential components of TCR signaling required to mount a successful immune response. Although defects in either T cell–specific Tec kinase, Itk or Rlk, have only mild to moderate effects on T cell function, elimination of both kinases resulted in a profound loss of mature T cell function in vitro and in vivo. Our data show that nonreceptor tyrosine kinases are important not only for initiation of antigen-driven responses but also for downstream propagation of these signals. The biochemical defects reported here resemble those observed in Slp-76–deficient cells (*18*), suggesting that Tec kinases and Slp-76 are part of a complex that activates PLC-γ. The requirement for multiple Tec kinases in TCR signaling is also intriguing, particularly given differential sensitivities of Rlk and Itk activation to PI3K inhibition (*7*). Products of PI3K are required for

Btk activation of sustained Ca^{2+} mobilization in response to secretory immunoglobulin M (*19*). Thus, Rlk, a distinct Tec kinase that functions independently of PI3K, may provide a second level of regulation to antigen receptor signaling pathways in T cells.

Current models suggest that immune responses in lymphocytes are exquisitely controlled, requiring multiple finely tuned levels of activation (*20*). Thus, the Tec kinases, unlike the more proximally acting Lck and Zap-70, may not serve as primary triggers of the immune response but instead may further refine the strength of lymphocyte signaling by acting as critical modulators of PLC-γ and downstream effectors.

References and Notes

1. A. Weiss and D. R. Littman, *Cell* **76**, 263 (1994); R. L. Wange and L. E. Samelson, *Immunity* **5**, 197 (1996).
2. D. B. Straus and A. Weiss, *Cell* **70**, 585 (1992); B. L. Williams *et al.*, *Mol. Cell. Biol.* **18**, 1388 (1998).
3. S. Desiderio and J. D. Siliciano, *Chem. Immunol.* **59**, 191 (1994).
4. D. J. Rawlings and O. N. Witte, *Semin. Immunol.* **7**, 237 (1995).
5. M. F. Bachmann, D. R. Littman, X. C. Liao, *J. Virol.* **71**, 7253 (1997).
6. R. N. Haire *et al.*, *Hum. Mol. Genet.* **3**, 897 (1994); Q. Hu *et al.*, *J. Biol. Chem.* **270**, 1928 (1995); C. L. Sommers *et al.*, *Oncogene* **11**, 245 (1995).
7. J. Debnath *et al.*, *Mol. Cell. Biol.* **19**, 1498 (1999).
8. E. Schaeffer, J. Debnath, P. Schwartzberg, unpublished results.
9. X. C. Liao and D. R. Littman, *Immunity* **3**, 757 (1995).
10. The near normal mature T cell numbers in $rlk^{-/-}itk^{-/-}$ mice may result from differential requirements for Itk and Rlk during T cell development versus mature T cell activation or compensatory expression of Tec in thymocytes. However, preliminary evidence from TCR transgenic mice suggests that combined deficiency of Rlk and Itk decreases selection processes with a switch from negative to positive selection that may account for increased cellularity in $rlk^{-/-}itk^{-/-}$ mice relative to $itk^{-/-}$ mice (*8*).
11. K. Q. Liu, S. C. Bunnell, C. B. Gurniak, L. J. Berg, *J. Exp. Med.* **187**, 1721 (1998).
12. M. J. Lenardo, *Semin. Immunol.* **9**, 1 (1997).
13. D. Y. Noh, S. H. Shin, S. G. Rhee, *Biochim. Biophys. Acta* **1242**, 99 (1995).
14. O. Sozeri *et al.*, *Oncogene* **7**, 2259 (1992); W. Kolch *et al.*, *Nature* **364**, 249 (1993).
15. Graded biochemical defects were observed in mutant cells, with $rlk^{-/-}$ appearing similar to wild-type cells and $itk^{-/-}$ more closely resembling the $rlk^{-/-}itk^{-/-}$ phenotype.
16. MAP kinase activation in T lymphocytes also occurs through GRB-2–mediated pathways (*21*). However, tyrosine-phosphorylated proteins bound by GRB-2's SH2 domain, including Cbl, Slp-76, and LAT (*21*, *22*), were normal in mutant cells (*8*), suggesting intact GRB-2–mediated signals.
17. T. M. Scharton-Kersten and A. Sher, *Curr. Opin. Immunol.* **9**, 44 (1997); E. Y. Denkers *et al.*, in *Host Response to Intracellular Pathogens*, S. H. E. Kaufman, Ed. (Landes, Austin, TX, 1997), pp. 167–181.
18. D. Yablonski, M. R. Kuhne, T. Kadlecek, A. Weiss, *Science* **281**, 413 (1998).
19. A. M. Scharenberg and J. P. Kinet, *Cell* **94**, 5 (1998).
20. J. Sloan-Lancaster and P. M. Allen, *Annu. Rev. Immunol.* **14**, 1 (1996); J. Madrenas and R. N. Germain, *Semin. Immunol.* **8**, 83 (1996).
21. D. Cantrell, *Annu. Rev. Immunol.* **14**, 259 (1996).
22. W. Zhang, J. Sloan-Lancaster, J. Kitchen, R. P. Trible, L. E. Samelson, *Cell* **92**, 83 (1998).
23. Purified splenocytes (5×10^6) were stimulated for indicated times with plate-bound 2C11 (7.5 μg/ml), lysed in 1% Triton and 0.1% SDS in phosphate-buffered saline with protease inhibitors (Boehringer Mannheim) and sodium vanadate, and immunoprecipitated with either anti–TCR zeta chain (gift of L. Samelson) or anti–Zap-70 (Upstate). Immune complexes were resolved by 10% SDS–polyacrylamide gel electrophoresis (SDS-PAGE) and immunoblotted with anti-phosphotyrosine (4G10 Upstate).
24. pMC1neo and multiple stop codons were inserted into the Kpn I site of *rlk* (encoding the start of the SH2 domain) with 6-kb upstream and 3-kb downstream sequences, followed by herpes simplex virus thymidine kinase (HSV-TK). The construct was electroporated into TC1 ES cells and G418-gancyclovir–resistant colonies screened by Southern (DNA) blot analyses with Hind III and a flanking 3′ probe. Gene disruption at the 5′ end was confirmed with an internal probe.
25. Splenocytes were stimulated with PMA (10 ng/ml) and ionomycin (1 μg/ml) for 24 hours to ensure equal proliferation, washed, and grown with IL-2 for 3 days. Cells were restimulated with anti-CD3ε (2C11) for 24 hours, and cell viability was determined by flow cytometry.
26. Internal Ca^{2+} in purified T cells (5×10^6 per milliliter) loaded with Fluo-3-AM (5 μg/ml) and Fura-Red-AM (5 μg/ml) (Molecular Probes, Eugene, OR) (*13*) was analyzed with MultiTime Kinetic Experiment Analysis Software (Phoenix Flow Systems, San Diego, CA), and data were expressed as percentage responding relative to unstimulated cells.
27. Purified splenic T cells (4.0×10^7) were stimulated (*23*) and examined by IP_3 Radioreceptor Assay Kit (NEN Life Science).
28. E. Y. Denkers *et al.*, *J. Immunol.* **159**, 1903 (1997).

29. We thank L. Samelson, J. O'Shea, J. Dodson, and R. Nussbaum for comments; A. Wynshaw-Boris, C. Canna, and D. Bernards for assistance with ES cells; S. Anderson for flow cytometry; and M. Czar, A. Venegas, W. Hively, G. Elliot, M. Chamorro, L. Brody, E. Arnold, M. Erdos, L. Zheng, B. Combediere, and R. Siegel. Animal care was in accordance with NIH guidelines. This work was initiated in the laboratory of M.J.L., continued in the laboratory of H.E.V., and completed in the laboratory of P.L.S. E.M.S. and J.D. are Howard Hughes Medical Institute–NIH Research Scholars.

18 December 1998; accepted 15 March 1999

Efficient Persistence of Extrachromosomal KSHV DNA Mediated by Latency-Associated Nuclear Antigen

Mary E. Ballestas,[1] Pamela A. Chatis,[2,3] Kenneth M. Kaye[1]*

Primary effusion lymphoma (PEL) cells harbor Kaposi's sarcoma–associated herpesvirus (KSHV) episomes and express a KSHV-encoded latency-associated nuclear antigen (LANA). In PEL cells, LANA and KSHV DNA colocalized in dots in interphase nuclei and along mitotic chromosomes. In the absence of KSHV DNA, LANA was diffusely distributed in the nucleus or on mitotic chromosomes. In lymphoblasts, LANA was necessary and sufficient for the persistence of episomes containing a specific KSHV DNA fragment. Furthermore, LANA co-localized with the artificial KSHV DNA episomes in nuclei and along mitotic chromosomes. These results support a model in which LANA tethers KSHV DNA to chromosomes during mitosis to enable the efficient segregation of KSHV episomes to progeny cells.

Kaposi's sarcoma (KS)–associated herpesvirus or human herpesvirus–8 likely plays an important role in KS pathogenesis because KSHV seropositivity precedes KS and KSHV DNA is found in almost all KS lesions, whether or not there is a coexisting human immunodeficiency virus infection (*1*). KSHV is also associated with lymphoproliferative disorders, including PELs and multicentric Castleman's disease (*2*, *3*).

Similar to the gamma-1 herpesvirus Epstein-Barr virus (EBV), KSHV infection in tumor tissue or in lymphoma-derived cell lines is predominantly latent. Latently infected cells have multiple copies of circularized KSHV DNA maintained as episomes (*2*–*4*). The EBV nuclear antigen–1 (EBNA1) protein mediates efficient episome persistence through a cis-acting 1.8-kb EBV DNA sequence, which is termed the origin of plasmid replication (oriP) (*5*, *6*). Herpesvirus saimiri (HVS) also has a cis-acting sequence that enables the efficient persistence of episomes in HVS-infected cells (*7*). However, KSHV has no obvious homology to the EBV or HVS cis-acting DNA, and a trans-acting EBNA1 homolog or analog has not been identified in HVS or in other gamma-2 herpesviruses.

KSHV open reading frame (ORF) 73 encodes the latency-associated nuclear antigen (LANA, LNA, or LNA1), which is predicted to be 1162 amino acids, and lacks a known function (*1*, *8*, *9*). A homologous ORF exists in other gamma-2 herpesviruses (*10*). LANA is

[1]Department of Medicine, Channing Laboratory, Brigham and Women's Hospital, Harvard Medical School, 181 Longwood Avenue, Boston, MA 02115, USA. [2]Department of Medicine, Beth Israel Deaconess Medical Center, Harvard Medical School, 330 Brookline Avenue, Boston, MA 02215, USA. [3]NEN Life Science Products, 549 Albany Street, Boston, MA 02118, USA.

*To whom correspondence should be addressed. E-mail: kkaye@rics.bwh.harvard.edu